



# Experimental and theoretical assessment of selected pollutants treated with gamma radiation and hydrogen peroxide

Ayşenur Genç<sup>a</sup>, Ece Ergun<sup>b,\*</sup>, Alper Fitoz<sup>c</sup>, Ömer Kantoğlu<sup>b</sup>, Mahir İnce<sup>d</sup>, Orhan Acar<sup>a</sup>

<sup>a</sup> Gazi University, Department of Chemistry, Ankara, Turkey

<sup>b</sup> Turkish Energy, Nuclear and Mineral Research Agency, Nuclear Energy Research Institute, Ankara, Turkey

<sup>c</sup> Ankara University, Department of Chemistry, Ankara, Turkey

<sup>d</sup> Gebze Technical University, Department of Environmental Engineering, Kocaeli, Turkey

## ARTICLE INFO

Handling Editor: Dr. Jay Laverne

### Keywords:

Ionizing radiation  
Hydrogen peroxide  
Organic pollutants  
Fukui functions  
Dual descriptor  
Density functional theory

## ABSTRACT

Degradation of ibuprofen, triclosan, diclofenac, and ketoprofen in real wastewater effluent by gamma radiation/hydrogen peroxide was investigated on the basis of removal efficiencies, G-values, and kinetics. Gamma irradiation was performed using a <sup>60</sup>Co source irradiator in the presence of different concentrations of hydrogen peroxide. The analyses of the pollutants were performed before and after irradiation treatment using a Liquid Chromatography-Mass Spectrometry (LC-MS) system. The addition of 0.5% hydrogen peroxide resulted in an enhanced removal efficiency of the target pollutants (93.92% for ibuprofen, 99.47% for triclosan, 86.65% for diclofenac, and 86.32% for ketoprofen) compared with the performance of the gamma irradiation process alone. The rate constants (k) of ibuprofen, triclosan, diclofenac, and ketoprofen increased by 1.42, 2.38, 1.38, and 3.37 times with 0.5% hydrogen peroxide addition, respectively. Moreover, the 90% decomposition of the target pollutants was achieved at lower doses in the gamma-ray/hydrogen peroxide system in comparison with the gamma treatment without hydrogen peroxide. Fukui functions and dual descriptor were calculated using density functional theory (DFT) to investigate the sensitivity of the target pollutants to hydroxyl radical attacks, to identify the initial reaction pathway, and to predict the degradation by-products. The findings were consistent with literature mechanisms and observed by-products.

## 1. Introduction

Water pollution is one of the global problems that threaten the future of humanity. In today's world, indirect and direct discharges of pollutants into water bodies without appropriate treatment cause water pollution all over the world. Conventional wastewater treatment plants have the objective of reducing pollution levels to meet the permitted limits set by national regulatory authorities and to adhere to international criteria that allow the safe discharge or reuse of treated wastewater. However, some compounds are poorly removed during the wastewater treatment process, meaning they commonly end up in natural waters. Organic compounds previously not recognized or regarded as important in terms of their distribution and concentration that are now being more widely detected in aquatic environments are called emerging organic pollutants (EOPs). These compounds include a wide array of different compounds, such as pharmaceuticals, personal care products, surfactants, plasticizers, and various industrial additives,

which have been found to cause significant and lasting harm to the environment and human health. EOPs can have a lethal impact on the endocrine systems of humans and wildlife, even when present in trace quantities (µg/L or ng/L) (Wang and Chu, 2016).

Several studies were carried out to evaluate the feasibility of utilizing ionizing radiation (gamma-rays or electrons) to eliminate persistent pollutants and disinfect treated water and sludge. The findings of these investigations suggest that the use of ionizing radiation treatment holds significant potential from both a technical and economic standpoint (Abdel Rahman and Hung, 2020). Irradiation facilities can be built as add-on systems to the conventional wastewater treatment plant. Wastewater irradiators can provide extremely high treatment efficiencies in contrast to many other advanced oxidation process (AOP) technologies. Radiation processing in wastewater treatment, similar to other AOPs, relies on the oxidation of organic pollutants through hydroxyl radicals. Moreover, the production of reactive reducing species in addition to hydroxyl radicals during the radiolysis of water facilitates

\* Corresponding author.

E-mail address: [ece.ergun@tenmak.gov.tr](mailto:ece.ergun@tenmak.gov.tr) (E. Ergun).

<https://doi.org/10.1016/j.radphyschem.2024.112473>

Received 13 September 2024; Received in revised form 6 December 2024; Accepted 10 December 2024

Available online 15 December 2024

0969-806X/© 2024 Elsevier Ltd. All rights are reserved, including those for text and data mining, AI training, and similar technologies.

the degradation of several types of EOPs through oxidation and/or reduction pathways (Hina et al., 2021).

In our previous study (Genç et al., 2024), the effect of gamma radiation treatment on the different organic contaminants present in real wastewater effluent samples was investigated. Our validated analytical procedure revealed that the concentrations of the target EOPs were at sub- $\mu\text{g L}^{-1}$  levels. Compared to the literature data obtained from synthetic water samples, it was found that relatively high doses (10–30 kGy) were necessary to attain high removal efficiencies. This is primarily due to the competition between trace concentrations of EOPs and the other components present in real wastewater. The required high doses make the irradiation method expensive and time-consuming. Recently, the studies regarding gamma radiation in combination with different additives were performed to achieve a synergetic effect of degradation. Hydrogen peroxide, the most commonly used additive, has proven to be effective for the degradation of extensive aqueous contaminants as a potential source of hydroxyl radicals (Egerić et al., 2024). In their study, Chu et al. (2021) demonstrated that  $\text{H}_2\text{O}_2$  addition during gamma irradiation exhibited a synergetic effect on the removal of COD and antibiotics in the secondary effluent from an antibiotic wastewater treatment plant. In a separate study conducted by Shah et al. (2020), it was shown that when a 15  $\mu\text{M}$  Congo red solution was exposed to a dose of 1.184 kGy, 53% of the compound was degraded. However, the addition of  $\text{H}_2\text{O}_2$  significantly enhanced the degradation process, resulting in a remarkable 98% degradation under the same experimental conditions. The results reported by Iqbal and Bhatti (2015) showed that gamma radiation/ $\text{H}_2\text{O}_2$  treatment has the potential to mineralize and detoxify nonylphenol polyethoxylates at 15 kGy irradiation dose and 4.58%  $\text{H}_2\text{O}_2$ . Another study performed by Choi et al. (2010) revealed that the combination of gamma irradiation and  $\text{H}_2\text{O}_2$  remarkably increased the degradation efficiency of alachlor and the total organic carbon removal. Other studies on various organic compounds have demonstrated that  $\text{H}_2\text{O}_2$  is the predominant additive that facilitates degradation in the presence of gamma irradiation (Alkhuraiji et al., 2017; Jia-Tong et al., 2017; Huang et al., 2016; Yu et al., 2010). In the light of these studies, gamma radiation was coupled with hydrogen peroxide to accelerate the process by generating additional hydroxyl radicals and reduce the required dose for degradation in this work. Ibuprofen (IBU), triclosan (TCS), diclofenac (DCF), and ketoprofen (KET) were here selected as model EOPs. In our previous study, the maximum degradation efficiency was achieved for IBU at 10 kGy, TCS and DCF at 20 kGy, and KET at 30 kGy using gamma irradiation alone, therefore the synergetic effect of gamma irradiation and hydrogen peroxide on these contaminants was investigated at the lowest examined dose (10 kGy) in this study.

A reaction mechanism describes the process in which the reactants in a chemical reaction are transformed into products. Therefore, the reaction mechanism depends on the molecular structure, the functional groups in the molecule, and the characteristics of the incoming reagent. Since products of water radiolysis behave as either electrophiles or nucleophiles, it is important to identify the electron-rich and electron-poor regions of the molecule for the attack. Quantum mechanics-based approaches, such density functional theory (DFT), can be used alongside experimental findings to gain a deeper understanding of reaction mechanisms and provide mechanistic insight. Local reactivity descriptors (LRD) derived from DFT are employed to accurately characterize the reactivity site of molecules. The Fukui function, also known as the frontier function, is the most significant LRD that aids in comprehending the local reactivity and selectivity of a molecule. Different types of Fukui indices are prescribed for electrophilic ( $f^-$ ), nucleophilic ( $f^+$ ), and radical ( $f^0$ ) attacks (Pal and Chattaraj, 2023; Pucci and Angilella, 2022). The dual descriptor ( $f^{(2)}$ ), derived from the difference between the nucleophilic and electrophilic Fukui indices, is considered a more reliable LRD to measure site reactivity (Martínez-Araya, 2015). Therefore, these indices can be used to determine the reactivity of the target

EOPs with hydroxyl radicals. In recent studies, the condensed Fukui functions has been increasingly applied to calculate the reaction sites of organic pollutants with hydroxyl radicals (He et al., 2023; Rath et al., 2023; Dwinandha et al., 2022; Huo et al., 2021; Jia et al., 2016). However, these studies have certain limitations, as they do not comprehensively assess all the condensed Fukui functions and dual descriptor simultaneously. Therefore, the applicability of the condensed Fukui indices to evaluation the reactive sites and the initial reaction mechanism is still a challenge.

In this study, Fukui functions and dual descriptors of target EOPs (IBU, TCS, DCF, and KET) were also calculated to determine the local electrophilic, nucleophilic, and radical sites in order to evaluate the electrophilic hydroxyl radical attack regions and initial degradation pathways as well as predict the by-products. The findings were compared with the experimental observations and literature data to assess the consistency between theoretical calculations and experimental results, as well as the applicability of LRD.

## 2. Materials and methods

### 2.1. Chemicals and reagents

All chemical reagents utilized in this study were of high-purity analytical grade and employed without additional purification. Ibuprofen, triclosan, diclofenac, and ketoprofen (molecular structures are given in Fig. S1) were purchased from Sigma-Aldrich. A Milli-Q Gradient Water Purification system (Millipore, Billerica, MA, USA) was used to provide highly purified water.

Stock solutions of ibuprofen (0.0970 mmol  $\text{L}^{-1}$ ), triclosan (0.0691 mmol  $\text{L}^{-1}$ ), diclofenac (0.0675 mmol  $\text{L}^{-1}$ ), and ketoprofen (0.0786 mmol  $\text{L}^{-1}$ ) were prepared by individually dissolving the standards in acetonitrile. Then, these solutions were diluted with acetonitrile to prepare working solutions for the calibration graph.

Glass containers were used to collect the wastewater effluent samples from the Gebze wastewater treatment facility located in Kocaeli. These samples were then transported to the laboratory and were stored in the dark at a temperature of 4 °C for no more than one week before irradiation, and then immediately analyzed.

### 2.2. Gamma irradiation

The wastewater effluent samples were placed in 1 L glass bottles with screw-cap for gamma irradiation.  $\text{H}_2\text{O}_2$  was added into the vials before the irradiation, making the initial  $\text{H}_2\text{O}_2$  concentrations 0, 0.1, 0.5, and 1.0%. The initial pH of the samples was in the range of 7.0–7.2.

A  $^{60}\text{Co}$  irradiator (Ob-Servo Sanguis, acquired from the Institute of Isotopes Co., Ltd., Budapest, Hungary), located at the Nuclear Energy Research Institute in Ankara, Türkiye, was used to carry out the irradiation studies. At ambient temperature and without any additional treatment, the wastewater samples were exposed to irradiation in the presence of  $\text{H}_2\text{O}_2$  at a dose of 10 kGy (dose rate: 1.35 kGy  $\text{h}^{-1}$ ).

### 2.3. Analysis

The extraction of the target EOPs was carried out using a previously developed and validated method for wastewater samples (Genç et al., 2024). Scheme S1 provides a concise summary of the developed and validated extraction procedure for the target EOPs.

EOPs were analyzed before and after irradiation treatment utilizing a Waters Alliance 2695 HPLC system connected to a Waters Micromass ZQ 2000 single quadrupole mass spectrometer equipped with a XTerra® MS C18 (5  $\mu\text{m}$ , 150  $\times$  4.6 mm, Waters) column. The column and the auto-sampler were maintained at a temperature of 25 °C. The injection volume was 20  $\mu\text{L}$ . Target EOPs were ionized via electrospray ionization (ESI) in both positive and negative modes and quantified using selected ion monitoring (SIM) mode. The specific LC-ESI-MS operating settings

for identifying target EOPs are outlined in Table S1. The additional optimal parameters for mass spectrometry are a source temperature of 150 °C, a desolvation temperature of 300 °C, a capillary voltage of 3.5 kV, a desolvation gas flow of 500 L h<sup>-1</sup>, and a cone gas flow of 50 L h<sup>-1</sup>. The data collecting and processing were performed using Masslynx v4.1 software (Genç et al., 2024).

The pH and conductivity of the samples were measured using a Mettler Toledo SevenGo SG2 pH meter connected to a Mettler Toledo InLab®413 pH electrode, and a Mettler Toledo SG3 conductivity meter paired with an InLab®738 conductivity probe (Mettler-Toledo, Switzerland).

The removal efficiencies were determined by calculating the percentage reduction in EOP concentrations.

$$\text{Removal efficiency (\%)} = [(C_0 - C) / C_0] \times 100 \quad \text{Eq. (1)}$$

C<sub>0</sub> and C represent the concentrations of the target compound before and after the irradiation, respectively.

The G-values were calculated according to the following equation (Boujelbane et al., 2022; Kantoğlu and Ergun, 2015, 2016):

$$G (\mu\text{mol J}^{-1}) = \frac{6.023 \times 10^{23} \times \text{chemical yield}}{6.24 \times 10^{16} \times D (\text{Gy})} \quad \text{Eq. (2)}$$

D denotes the absorbed dose, while chemical yield indicates the change in concentration of the target compound ( $\Delta C$ ).  $6.023 \times 10^{23}$  is the Avogadro's number and  $6.24 \times 10^{16}$  the conversion factor from Gy to 100 eV L<sup>-1</sup>.

The degradation kinetic rates of the target EOPs were calculated using dose dependent pseudo first-order kinetic reaction model, which is described as (Boujelbane et al., 2022):

$$-\ln[C / C_0] = kD \quad \text{Eq. (3)}$$

where C<sub>0</sub> is the initial concentration of the target molecules before irradiation, C is the residual concentration of the target molecules after irradiation; D is the absorbed dose (kGy); and k is the rate constant (kGy<sup>-1</sup>).

Rate constants were employed to calculate the absorbed doses necessary for achieving 90% degradation (D<sub>0.9</sub>) of the target molecules (Eq. (4)) (Boujelbane et al., 2022):

$$D_{0.9} = \ln 10 / k \quad \text{Eq. (4)}$$

#### 2.4. Theoretical calculations

The geometrical optimization was performed using the Gaussian 09 software (Frisch et al., 2009), applying Density Functional Theory (DFT) with Becke's three-parameter exchange function, the Lee-Yang-Parr nonlocal correlation functional (B3LYP), and a 6-31G (d, p) basis set in solvent (water) mode (Fitöz et al., 2023).

In DFT, Fukui functions are descriptors that enable the identification of the most reactive regions on a molecule. The Fukui concept is defined as the variation in the electronic density due to the change in the electron number at fixed external potential (Parr and Yang, 1984; Pucci and Angilella, 2022):

$$f(\vec{r}) = \left( \frac{\partial \rho(\vec{r})}{\partial N} \right)_{V(\vec{r})} \quad \text{Eq. 5}$$

where  $f(\vec{r})$  is Fukui function,  $\rho(\vec{r})$  is electron density of a certain atom, N is total number of electrons in the molecule, V is the external potential.

Equation (5) provides three reaction indices (three Fukui functions):

$$f^-(\vec{r}) = \rho_N(\vec{r}) - \rho_{N-1}(\vec{r}) \approx \rho_{\text{HOMO}}(\vec{r}) \quad \text{Eq. 6}$$

$$f^+(\vec{r}) = \rho_{N+1}(\vec{r}) - \rho_N(\vec{r}) \approx \rho_{\text{LUMO}}(\vec{r}) \quad \text{Eq. 7}$$

$$f^0(\vec{r}) = [\rho_{N+1} - \rho_{N-1}] / 2 \quad \text{Eq. 8}$$

where  $\rho_N$ ,  $\rho_{N+1}$  and  $\rho_{N-1}$  represent the electron density of the system in the original state (N electrons), combined with one electron state (N+1 electrons) and ionized with one electron state (N-1 electrons), respectively. Therefore, the chemical meaning of  $f^-(\vec{r})$  is the capability of the molecule to donate an electron (for electrophilic attack), and  $f^+(\vec{r})$  is the capability of accepting an electron (for nucleophilic attack).  $f^0(\vec{r})$  represents radical reactivity.

Analyzing site selectivity using these local ( $\vec{r}$ ) dependent parameters is challenging. To tackle this problem, Yang and Mortier (1986) made independent calculations for the corresponding (N - 1), N, and (N + 1) electron systems for the atomic site k of the molecule with the same molecular geometry (condensed-to-atom variants) (Chattaraj and Roy, 2007). Therefore, the condensed Fukui functions can be written by replacing the associated electron densities by the respective electron populations (q<sub>k</sub>):

$$\text{Electrophilic attack : } f^- = q(N) - q(N-1) \quad \text{Eq. 9a}$$

$$\text{Nucleophilic attack : } f^+ = q(N+1) - q(N) \quad \text{Eq. 10a}$$

$$\text{Radical attack : } f^0 = [q(N+1) - q(N-1)] / 2 \quad \text{Eq. 11a}$$

where q is atomic electron population (in this study Mulliken population analysis) in the original system with N electrons (neutral system), N+1 electrons (anionic system), N-1 electrons (cationic system) (Pal and Chattaraj, 2023; Sakr et al., 2022; Martínez-Araya, 2015).

As the electron density varies with the number of electrons that are present in a certain region, the condensed Fukui function can be defined as a simplified version of the Fukui function for the atoms. In this way, each atom has an exact value, which makes it easy to compare the magnitude of the Fukui function at different sites at a quantitative level. Therefore, the atom with a larger Fukui index value is preferable for the attacks. Since the values of the Fukui function are related to the electron density of the frontier orbitals (HOMO and LUMO) they should be positive. However, in some cases negative values are found, which can be explained by orbital relaxation effects (Melin et al., 2007). The negative values were also ascribed to low HOMO- and LUMO-electron density that result in an unexpected change in electron density (Zamora et al., 2021).

The condensed dual descriptor, proposed as a more precise indicator (Martínez-Araya, 2015), was utilized to better investigate the electrophilic and nucleophilic sites. The condensed dual descriptor has been defined as:

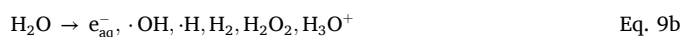
$$f^{(2)} = f^+ - f^- \quad \text{Eq. 12a}$$

where  $f^+$  and  $f^-$  are condensed nucleophilic and electrophilic Fukui functions. (Martínez-Araya et al., 2013). The condensed dual descriptor allows one to obtain simultaneously the preferably sites for nucleophilic attacks ( $f^{(2)} > 0$ ) and the preferably sites for electrophilic attacks ( $f^{(2)} < 0$ ).

### 3. Results and discussion

#### 3.1. Effect of H<sub>2</sub>O<sub>2</sub> addition on the degradation of EOPs

The concentrations of the target EOPs (IBU, TCS, KET, and DCF) in the real wastewater effluent investigated in this study were at nmol L<sup>-1</sup> level (1.474, 1.958, 3.709, and 0.767 nmol L<sup>-1</sup>, respectively). The degradation of organic contaminants in dilute aqueous solutions is initiated by the primary products of water radiolysis (Eq. (9)), namely •OH, e<sub>aq</sub><sup>-</sup>, and •H (Wojnárovits and Takács, 2016; Buxton et al., 1988):



The products of water radiolysis, e<sub>aq</sub><sup>-</sup> and •H, are strong reducing

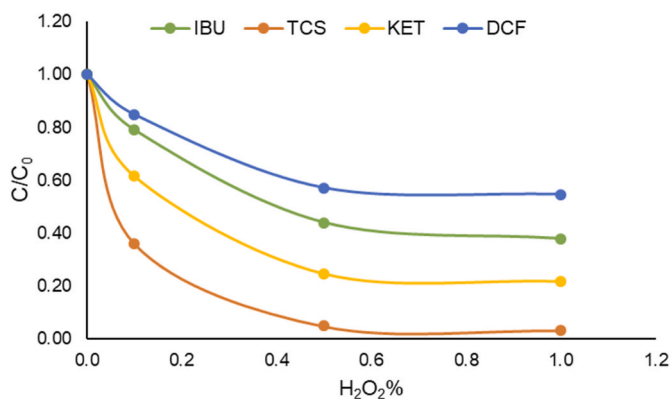


Fig. 1. Effect of absorbed dose (10 kGy) and initial H<sub>2</sub>O<sub>2</sub> concentration on IBU, TCS, DCF, and KET removal.

Table 1

Variation of removal efficiency and G-value of the target EOPs irradiated at 10 kGy in the presence of 0.1, 0.5, and 1.0% H<sub>2</sub>O<sub>2</sub>.

EOPs	Dose/H <sub>2</sub> O <sub>2</sub> kGy/%	Removal Efficiency %	G-value μmol J <sup>-1</sup>
IBU	10/0	86.10 ± 0.93	1.225 ± 0.013
	10/0.1	89.25 ± 1.65	1.270 ± 0.023
	10/0.5	94.06 ± 0.44	1.338 ± 0.006
	10/1.0	94.72 ± 0.49	1.347 ± 0.007
TCS	10/0	89.06 ± 1.00	1.683 ± 0.019
	10/0.1	96.12 ± 0.75	1.817 ± 0.014
	10/0.5	99.52 ± 0.20	1.881 ± 0.004
	10/1.0	99.64 ± 0.11	1.883 ± 0.002
DCF	10/0	76.67 ± 4.36	0.567 ± 0.032
	10/0.1	80.21 ± 0.65	0.593 ± 0.005
	10/0.5	86.79 ± 1.25	0.642 ± 0.009
	10/1.0	87.23 ± 0.62	0.645 ± 0.005
KET	10/0	44.86 ± 1.65	1.606 ± 0.059
	10/0.1	72.48 ± 1.44	2.594 ± 0.052
	10/0.5	86.32 ± 0.29	3.090 ± 0.010
	10/1.0	87.91 ± 0.46	3.147 ± 0.016

agents, whereas •OH is highly reactive and capable of oxidizing a wide range of compounds. Nevertheless, as our irradiation experiments were not conducted under strictly anaerobic conditions, the e<sub>aq</sub><sup>-</sup> and •H species in the solution would readily convert into less reactive •HO<sub>2</sub> and •O<sub>2</sub><sup>-</sup> via Eqs. (10) and (11) (Woods and Pikaev, 1994),



•O<sub>2</sub><sup>-</sup> is a weak reductant, while •HO<sub>2</sub> is a moderate oxidant. However, in neutral solutions, these species gradually vanish through slow radical-radical reactions, leading to the formation of H<sub>2</sub>O<sub>2</sub> (Eqs. (12) and (13)). As a result, they may not play a direct role in the degradation of organic pollutants (Wojnárovits and Takács, 2016). Consequently, it was proposed that the hydroxyl radical is the main reactive intermediate responsible for the degradation of the target EOPs.



Hydroxyl radicals exhibit high reactivity due to their instability, leading to rapid reactions with organic molecules. These reactions involve the abstraction of hydrogen from C–H bonds (H-abstraction also occurs from the hydroxyl group of the alcohol, albeit with a relatively

Table 2

Gamma radiation-induced EOP kinetic rate constants (k) and dose required for 90% decomposition (D<sub>0.9</sub>).

EOPs	Initial concentration nmol L <sup>-1</sup>	Dose/H <sub>2</sub> O <sub>2</sub> kGy/%	Rate constant (k) kGy <sup>-1</sup>	D <sub>0.9</sub> kGy
IBU	1.474	10/0	0.195 ± 0.004	11.79 ± 0.23
		10/0.5	0.285 ± 0.007	8.08 ± 0.20
TCS	1.958	10/0	0.222 ± 0.009	10.40 ± 0.43
		10/0.5	0.539 ± 0.043	4.28 ± 0.34
DCF	0.767	10/0	0.146 ± 0.019	15.86 ± 0.21
		10/0.5	0.203 ± 0.009	11.46 ± 0.32
KET	3.709	10/0	0.059 ± 0.002	38.70 ± 0.44
		10/0.5	0.198 ± 0.003	11.51 ± 0.36

low probability) or electrophilic addition to double bonds, which generate carbon-centered radicals. These carbon-centered radicals react with hydroxyl radicals or dissolved oxygen to form by-products. Moreover, further reactions can lead to complete mineralization (Wojnárovits and Takács, 2016; Buxton et al., 1988).

In our previous study, the efficient radiolytic decomposition of the target EOPs in real wastewater effluent was achieved at high doses (10–30 kGy) (Genç et al., 2024). Due to their nonselective nature, hydroxyl radicals react with both target molecules and matrix components in the sample. Additionally, radical-radical recombination reactions in highly dilute solutions could also play a role in the quenching process of hydroxyl radicals (Wang et al., 2019; Woods and Pikaev, 1994). All of these factors led to a decrease in the concentration of hydroxyl radicals available for reacting with the target EOPs, resulting in an increase in the required dose for efficient degradation. In order to enhance the degradation efficiency of these contaminants at the lowest examined dose (10 kGy), synergetic effect of gamma irradiation and hydrogen peroxide was investigated in this study.

Gamma irradiation-induced degradation of target EOPs in real wastewater effluent at different initial H<sub>2</sub>O<sub>2</sub> concentrations at a dose of 10 kGy was shown in Fig. 1 and Table 1. The results indicated that target EOPs were degraded efficiently with the addition of 0.1% and 0.5% H<sub>2</sub>O<sub>2</sub> concentrations. For 10 kGy/0.5% H<sub>2</sub>O<sub>2</sub> treatment, the removal efficiencies of IBU, TCS, DCF, and KET were found to be 93.92, 99.47, 86.65, and 86.32%, respectively. After gamma irradiation at a dose of 10 kGy, no significant difference was found in the removal efficiencies and G-values of samples containing 0.5% and 1.0% H<sub>2</sub>O<sub>2</sub>. In order to gain a deeper comprehension of the degradation process of target EOPs through gamma irradiation/H<sub>2</sub>O<sub>2</sub> treatment, kinetic rate constants were calculated and compared with the constants obtained from gamma irradiation treatment at a dose of 10 kGy without H<sub>2</sub>O<sub>2</sub> addition (Table 2).

The experimental results demonstrate that H<sub>2</sub>O<sub>2</sub> has a substantial impact on the removal efficiency, radiolytic yield (G-value), and degradation rate constants of the target EOPs. The addition of H<sub>2</sub>O<sub>2</sub> enhances the efficiency of pollutant removal by increasing the G-values and degradation rate constants (Tables 1 and 2). The 90% decomposition of the target EOPs was achieved at lower doses (D<sub>0.9</sub>) in the gamma-ray/H<sub>2</sub>O<sub>2</sub> system compared to the gamma-ray/H<sub>2</sub>O<sub>2</sub>-free system (Table 2).

The acceleration of the degradation of pollutants by adding H<sub>2</sub>O<sub>2</sub> to the aqueous solution, which provides more hydroxyl radical (Eqs. (14)

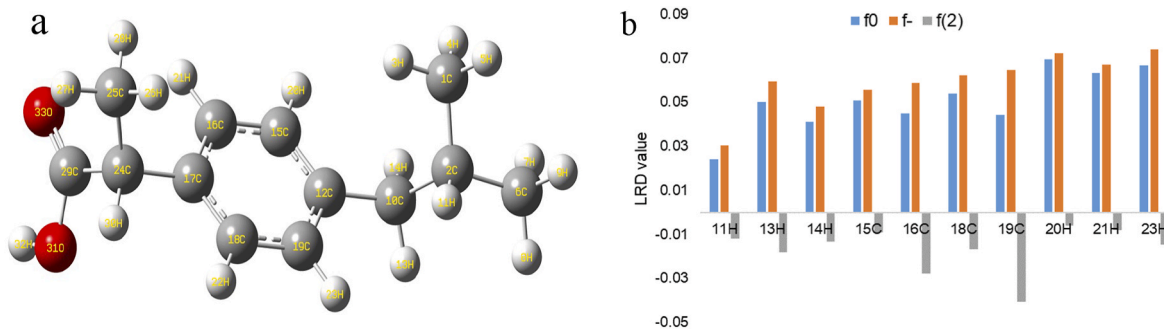


Fig. 2. a) Optimized geometry b) local reactivity descriptors of IBU.

and (15)) (Buxton et al., 1988), evidently shows that radiolytic degradation is more efficient under oxidative conditions.



On the other hand, 1.0%  $\text{H}_2\text{O}_2$  reduced the degradation efficiency of the target EOPs and inhibited the degradation process due to the excessive concentration of  $\text{H}_2\text{O}_2$ , which scavenges hydroxyl radicals to form hydroperoxy radicals (Eq. (16)) (Ibrahim et al., 2018; Zheng et al., 2011).



The rate constants and the  $\text{D}_{0.9}$  value are the most significant data that offer information regarding the yield of the radiolytic decomposition process. The results indicate that the addition of 0.5%  $\text{H}_2\text{O}_2$  has the greatest impact on the degradation of KET. The rate constant of KET exhibited a 3.37-fold increase in comparison to the gamma-ray/ $\text{H}_2\text{O}_2$ -free system. Conversely, the pollutant that is least affected can be identified as DCF, since its rate constant only increases by a factor of 1.38 (Table 2). However, the rate constants and  $\text{D}_{0.9}$  values depend on the concentration of the pollutant and have to therefore be assessed for a particular concentration level (Bojanowska-Czajka et al., 2015). Besides, the molecular structure of pollutants is an important parameter in determining their susceptibility to attack by hydroxyl radicals. At this point, the theoretical calculations (discussed in Section 3.2) can provide valuable information for the degradation process, particularly in predicting the by-products of pollutants.

### 3.2. Theoretical calculations

To evaluate the reactivity of a molecule, it is essential to assess the changes in its electronic density caused by the influence of an approaching reactant. Fukui functions are indicators for the change of electron density induced by the change of absolute electron number at a

fixed geometry and external potential and are very important descriptors in the DFT that are used for the identification of the most reactive sites on a molecule. The condensed Fukui functions allow to predict the susceptibility towards nucleophilic ( $f^+$  index), electrophilic ( $f^-$  index) and free radical ( $f^0$  index) attack for each atom as mentioned in Section 2.4. However, some nucleophilic sites on a molecule overlap with some electrophilic sites. Therefore, the issue arises: what is the nature of the region? Is it nucleophilic or electrophilic? The answer is given by the dual descriptor, which allows to remove this ambiguity. The condensed dual descriptor is determined by calculating the arithmetic difference between  $f^+$  and  $f^-$  indices. This additional approximation enhances the accuracy of describing the true nucleophilic and electrophilic sites on a molecule (Martínez-Araya, 2015).

In this study, the primary reactive species responsible for the degradation of the target EOPs were hydroxyl radicals, as mentioned in the experimental section. The highly reactive electrophilic hydroxyl radicals can rapidly and non-selectively attack sites of molecules with high electron density (Keen et al., 2014; Buxton et al., 1988). In this context, the regions with relatively high positive  $f^0$  and  $f^-$  values as well as relatively low negative  $f^{(2)}$  values were considered to be attacked by hydroxyl radicals.

#### 3.2.1. Ibuprofen

The structure of IBU is composed of an aromatic ring that connects an isobutyl group and a propanoic acid group. The optimized geometry of IBU is shown in Fig. 2a. All LRD values are given in Table S2.

The atoms with a high value of  $f^0$  characterized to be vulnerable to radical attack on IBU are 11H, 12C, 13H, 14H, 15C, 16C, 17C, 18C, 19C, 20H, 21H, 22H, 23H, 26H, 27H, 28H, 29C, 30H, 31O, 32H, and 33O (Table S2). Regarding  $f^-$  values, the same atoms have large values (Table S2), indicating that the electron population is located at these sites. However, 3H, 4H, 5H, 7H, 8H, 9H, 11H, 13H, 14H, 15C, 16C, 18C, 19C, 20H, 21H, and 23H atoms possess the negative  $f^{(2)}$  indices, meaning these atoms are the true sites for electrophilic attacks. Among them, the 11H, 13H, 14H, 16C, 18C, 19C, and 23H atoms with the

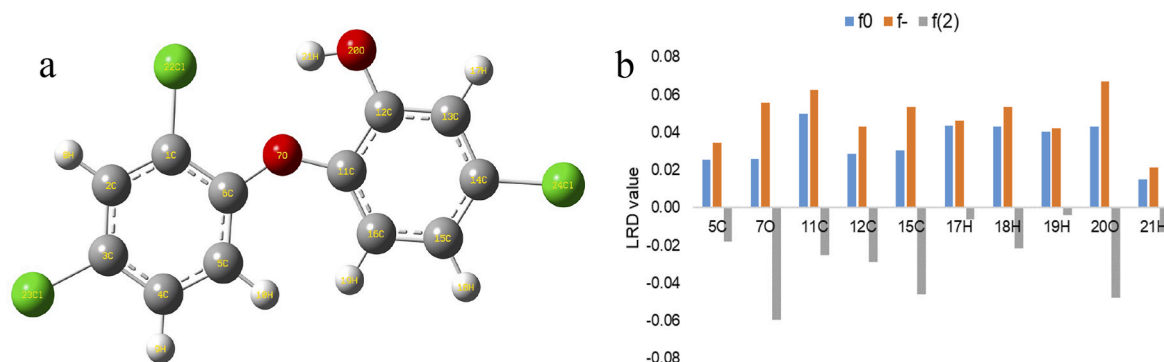


Fig. 3. a) Optimized geometry b) local reactivity descriptors of TCS.

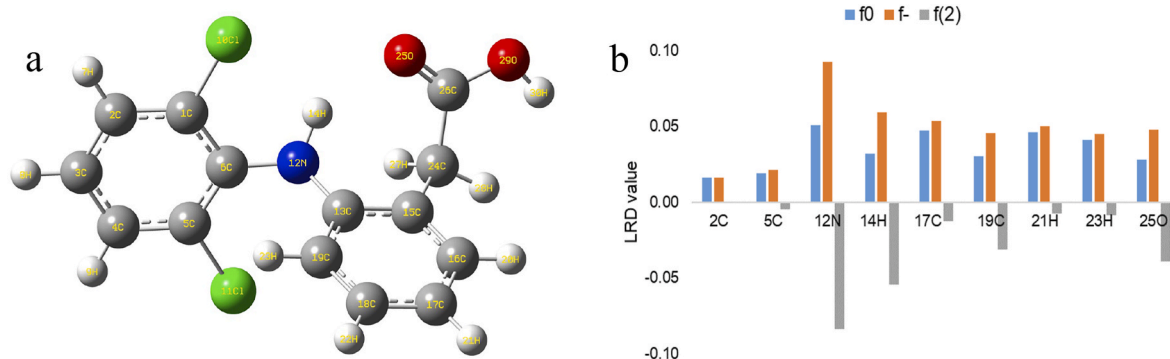


Fig. 4. a) Optimized geometry b) local reactivity descriptors of DCF.

highest  $f^0$  (Fig. 2b, blue bars) and  $f^-$  (Fig. 2b, orange bars) and the lowest  $f^{(2)}$  (Fig. 2b, gray bars) values are identified as the most probable locations for hydroxyl attack. As illustrated in Fig. 2b, the ring carbons are the most reactive atoms, suggesting that the addition of hydroxyl radical primarily occurs at these locations. Among them, 19C can be suggested as the most likely region for the hydroxylation due to the relatively lower  $f^{(2)}$  value. Besides, 11H bonded to tertiary 2C as well as 13H and 14H attached to benzylic 10C have considerably high  $f^0$  and  $f^-$  values. Moreover, these atoms have relatively low  $f^{(2)}$  indices, suggesting that these are the hydrogens that can be abstracted by an incoming electrophilic hydroxyl radical.

The major degradation products of IBU reported in the literature (Miranda et al., 2021; Illés et al., 2013; Zheng et al., 2011) were hydroxylated side chain molecules in the tertiary and/or secondary positions, as well as hydroxylated ring derivatives, confirming our findings. In this study, the proposed initial reaction route for the degradation of IBU under oxidative conditions is the hydroxylation of the aromatic ring, particularly at 19C position, which is in agreement with the literature reporting that this pathway is the most thermodynamically favorable (Miranda et al., 2021).

### 3.2.2. Triclosan

Triclosan is a chlorinated phenoxyphenol, containing a benzene ring, a phenolic ring, and three chlorine substituents, as depicted in Fig. 3a. The results of Fukui function calculations (Table S3) show that 5C, 7O, 11C, 12C, 15C, 18H, 20O, 21H, and 24Cl atoms with the relatively high  $f^0$  and  $f^-$  as well as the relatively low  $f^{(2)}$  values is the preferable sites for electrophilic hydroxyl radical attack (Fig. 3b).

Based on these results, the electrons are mostly located on the 7O site, meaning hydroxyl radicals can attack the ether bond region. When hydroxylation occurs on the 6C or 11C positions of TCS, TCS can be decomposed to yield 2,4-dichlorophenol and 4-chlorocatechol. The ether bond cleavage and detection of these by-products after the degradation of TCS was also reported previously (Zhang et al., 2021; Liu et al., 2020; Gao et al., 2016; Munoz et al., 2012). The notably higher positive  $f^0$  and  $f^-$  values and negative  $f^{(2)}$  value of 11C demonstrate that 11C is the more favorable site compared to 6C (see Table S3 for LRD values) for the hydroxylation reaction leading to the ether bond breakage.

This study reveals that 24Cl and 15C atoms exhibit comparatively high electron densities (see  $f^-$  and  $f^{(2)}$  values in Fig. 3b–Table S3), indicating that the hydroxyl radical can approach the TCS from this region. Therefore, this location can be suggested as the favorable initial reaction site. With this approach, the 15C atom can be the other candidate for the hydroxyl radical addition reaction pathway; in other words, hydroxylation of the aromatic ring. It has been reported that gamma irradiation has a dechlorination effect on TCS (Zhang et al., 2021; Wang et al., 2017). The suggested route involves the hydroxylation of TCS followed by the transformation into a dechlorinated

product through cleavage of chloride (Zhang et al., 2021; Song et al., 2012). Therefore, the addition of hydroxyl radical to the carbon-carbon double bond at position 15C and/or 5C could lead to the formation of TCS-OH, which may potentially trigger dechlorination.

Finally, the hydrogen abstraction from the phenolic hydroxyl group (20O–21H) by hydroxyl radical, leading to the dehydrogenated TCS radical, could give rise to the degradation of TCS, which has also been suggested based on quantum chemical calculations (Gao et al., 2014).

### 3.2.3. Diclofenac

The DCF molecule that has two aromatic rings connected with an amine group (Fig. 4a) possesses several reactive sites that can be attacked by the hydroxyl radicals. The hydroxyl radical attack is more likely to occur at the 12N, 14H, 17C, 19C, and 25O atoms due to their relatively high  $f^0$  and  $f^-$  as well as more negative  $f^{(2)}$  values compared to the other atoms (Fig. 4b–Table S4).

LRD analyses reveal that the primary electron-rich site of DCF can be attributed to 12N–14H bond region. Since the hydroxyl radical is preferentially attack at electron-dense sites, the hydroxyl radical attack on this position can initiate the cleavage of the C–N bond (12N–13C or 12N–6C). Thus, DCF gives two fragments (2,6-dichloroaniline and 2,6-dichlorophenol); depending on the spatial orientation of the hydroxyl radical attack (Banaschik et al., 2018; Nisar et al., 2016; Homlok et al., 2011). The mechanism suggested for this fragmentation is the addition of hydroxyl radical at ipso-position on the rings (13C or 6C). However, the electron density of these positions is relatively low (Table S4,  $f^+ > f^-$  and  $f^{(2)} > 0$ ). In addition, it was reported that the addition of hydroxyl radical to these sites is slightly less favorable than addition to the other ring carbons (Agopcan Cinar et al., 2017). This finding may potentially elucidate the reason why DCF is one of the least efficiently degraded molecule among the targeted EOPs in gamma-ray/ $H_2O_2$ -free system (Table 1).

The hydroxyl radical attack on the 17C and 19C positions could give rise to the formation of a hydroxylated DCF product. Previous investigations have observed the hydroxylated by-products of DCF and have proposed different sites for the addition of hydroxyl radical based on the substituent positioning effect (Zhuan and Wang, 2020; Bojanowska-Czajka et al., 2015; Yu et al., 2013; Homlok et al., 2011; Liu et al., 2011). This study reveals that the most probable hydroxylation sites are at 17C and 19C positions due to their relatively higher  $f^0$  and  $f^-$  values as well as lower  $f^{(2)}$  values, in comparison to the other carbons in the ring (Fig. 4b–Table S4). The addition of a hydroxyl group at the 19C position may result in the removal of a chlorine atom (loss of HCl from the primary phenolic product). Prior studies have reported the formation of a six-membered ring by-product resulting from cyclization caused by the elimination of HCl (Zhuan and Wang, 2020; Yu et al., 2013).

Finally, the carbonyl oxygen (25O) is one of the electron-rich sites among the atoms present in DCF. However, hydroxyl radical addition to the 25O = 26C double bond is not expected because the electron-

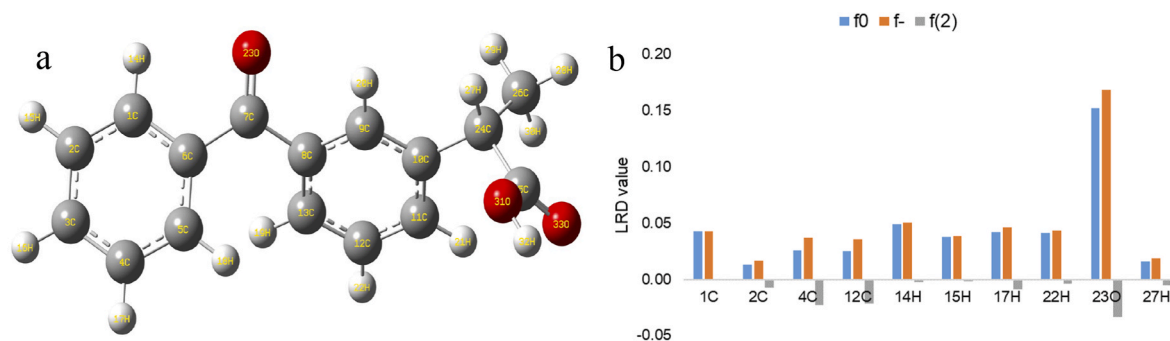


Fig. 5. a) Optimized geometry b) local reactivity descriptors of KET.

withdrawing property of oxygen makes the carbonyl carbon (26C) electron deficient, meaning that nucleophilic attack on this site is more likely (Table S4;  $f_{26C}^{(2)} > 0$ ).

### 3.2.4. Ketoprofen

Ketoprofen (Fig. 5a) is an oxo monocarboxylic acid, which offers two aromatic rings for hydroxyl radical addition and a tertiary side chain carbon (24C) for hydrogen abstraction. As illustrated in Fig. 5b and Table S5, the highest  $f^0$  and  $f^-$  as well as the lowest  $f^{(2)}$  values are located at 23O atom, indicating that this region is vulnerable to hydroxyl radical attack. When the  $7C = 23O$  double bond is considered, attacking the hydroxyl radical to the 7C atom and addition to the double bond is not expected due to the highly positive  $f^{(2)}$  value (Table S5). In the case of hydroxyl radical addition to the aromatic rings, the most preferred radical and electrophilic attack sites (highest  $f^0$  and  $f^-$  indices as well as lowest  $f^{(2)}$  value) among the ring carbons are 4C and 12C (Fig. 5b). It has been found that other aromatic carbons have very low electron density (Table S5). Based on the LRD values, it can be inferred that the electron withdrawing  $C=O$  group decreases the electron density of the ring carbons and negatively affects the hydroxyl radical addition reactions, which was also confirmed by the low degradation efficiency and rate observed in the gamma-ray/ $H_2O_2$ -free system (Table 1). When optimum  $H_2O_2$  concentration was employed with gamma irradiation, the process led to an increase in the number of hydroxyl radicals and enhanced the probability of the degradation reactions. The formation of hydroxylated by-products of KET was also reported in the literature (Martínez et al., 2013; Illés et al., 2012; Oturan et al., 1992).

On the other hand, the most available site for hydrogen abstraction reaction from the side chain is the tertiary 27H atom, which is found to be more susceptible to hydroxyl radical attack according to the LRD values (Fig. 5b and Table S5). The H-abstraction reaction from the side chain propionic acid group can give rise to the formation hydroxylation and subsequent decarboxylation to generate 3-hydroxyethyl benzophenone and 3-acetyl benzophenone, which are the common degradation products mentioned in the literature (Feng et al., 2014; Illés et al., 2014; Szabó et al., 2011).

Elucidating the by-product formation mechanisms is one of the most important steps in investigating the effect of ionizing radiation on the degradation of the target pollutants. However, real wastewater samples consist of a complex mixture of organic compounds, so following irradiation, determining the by-products is challenging due to the formation of various degradation products and the unavailability of their standards. This paper demonstrated that it was possible to predict the degradation mechanism and the by-products of the target contaminants by theoretical calculations and could be considered as an alternative approach. Theoretical calculations can also elucidate experimentally observed degradation efficiencies. For instance, this study suggested that the lower degradation efficiencies of DCF and KET molecules, compared to IBU and TCS, could be due to their limited sites for hydroxyl radical attack. However, it is well known that degradation

efficiency is concentration dependent; therefore, the different initial concentrations of the target pollutants in the wastewater have prevented us from drawing definitive conclusions. The interpretation of the degradation efficiencies based on the theoretical calculations must be evaluated for pollutants with the same concentration level.

## 4. Conclusion

This study demonstrated a high-efficiency gamma/ $H_2O_2$ -based degradation of ibuprofen, triclosan, diclofenac, and ketoprofen in real wastewater effluent. The maximum removal efficiencies of the target pollutants were achieved with a  $H_2O_2$  concentration of 0.5% at the absorbed dose of 10 kGy. The experimental findings of this study concluded that the addition of  $H_2O_2$  had a greater effect on the degradation of pollutants compared to gamma irradiation alone. In addition, the initial decomposition pathways were investigated via density functional theory. The by-products proposed based on the initial reaction routes derived from the theoretical calculations were in agreement with the experimental degradation products reported in the literature. Experimental data and quantum chemical calculations revealed that the reactions with the hydroxyl radicals mainly controlled the radiation-induced degradation of the target pollutants. This work also demonstrated the feasibility of LRD (Fukui function and dual descriptor) to predict the degradation and transformation mechanisms of contaminants in wastewater.

### CRedit authorship contribution statement

**Ayşenur Genç:** Writing – review & editing, Formal analysis, Data curation. **Ece Ergun:** Writing – original draft, Validation, Methodology, Investigation, Conceptualization. **Alper Fitoz:** Visualization, Software, Resources, Data curation. **Ömer Kantoğlu:** Writing – review & editing, Project administration, Methodology, Conceptualization. **Mahir İnce:** Supervision, Resources, Conceptualization. **Orhan Acar:** Writing – review & editing, Supervision, Methodology.

### Declaration of competing interest

The authors declare that they have no known competing financial interests or personal relationships that could have appeared to influence the work reported in this paper.

### Acknowledgements

This research has been funded by the International Atomic Energy Agency (IAEA) through the project on Radiation-Based Technologies for the Treatment of Emerging Organic Pollutants (CRP 23791) and the Turkish Energy, Nuclear and Mineral Research Agency (TENMAK) for Irradiation Applications and Research (A4.H1.F12). This study is a component of Ms. Ayşenur Genç's doctoral thesis. This research comprises a part of Ms. Ayşenur Genç's PhD thesis. Ms. Genç also received

support through the YÖK 100/2000 PhD scholarship program-02.01.02 in Molecular Pharmacology and Drug Investigation. The authors are thankful to Prof. Dr. Elif İnce for constant motivation and support (TÜBİTAK-115Y609 and TÜBİTAK-122Y377).

## Appendix A. Supplementary data

Supplementary data to this article can be found online at <https://doi.org/10.1016/j.radphyschem.2024.112473>.

## Data availability

Data will be made available on request.

## References

- Abdel Rahman, R.O., Hung, Y.-T., 2020. Application of ionizing radiation in wastewater treatment: an overview. *Water* 12, 19. <https://doi.org/10.3390/w1201019>.
- Agopcan Cinar, S., Ziyilan-Yavaş, A., Catak, S., Ince, N.H., Aviyente, V., 2017. Hydroxyl radical-mediated degradation of diclofenac revisited: a computational approach to assessment of reaction mechanisms and by-products. *Environ. Sci. Pollut. Res.* 24, 18458–18469. <https://doi.org/10.1007/s11356-017-9482-7>.
- Alkhurairi, T.S., Boukari, S.O.B., Alfadhl, F.S., 2017. Gamma irradiation-induced complete degradation and mineralization of phenol in aqueous solution: effects of reagent. *J. Hazard Mater.* 328, 29–36. <https://doi.org/10.1016/j.jhazmat.2017.01.004>.
- Banaschik, R., Jablonowski, H., Bednarski, P.J., Kolb, J.F., 2018. Degradation and intermediates of diclofenac as instructive example for decomposition of recalcitrant pharmaceuticals by hydroxyl radicals generated with pulsed corona plasma in water. *J. Hazard Mater.* 342, 651–660. <https://doi.org/10.1016/j.jhazmat.2017.08.058>.
- Bojanowska-Czajka, A., Kciuk, G., Gumiela, M., Borowiecka, S., Nałęcz-Jawecki, G., Koc, A., Garcia-Reyes, J.F., Solpan, Ozbay D., Trojanowicz, M., 2015. Analytical, toxicological and kinetic investigation of decomposition of the drug diclofenac in waters and wastes using gamma radiation. *Environ. Sci. Pollut. Res.* 22, 20255–20270. <https://doi.org/10.1007/s11356-015-5236-6>.
- Boujelbane, F., Nasr, K., Sadaoui, H., Bui, H.M., Gantri, F., Mzoughi, N., 2022. Decomposition mechanism of hydroxychloroquine in aqueous solution by gamma irradiation. *Chem. Pap.* 76, 1777–1787. <https://doi.org/10.1007/s11696-021-01969-1>.
- Buxton, G., Greenstock, C., Helman, W.P., Ross, A.B., 1988. Critical review of rate constants for reactions of hydrated electrons, hydrogen atoms and hydroxyl radicals (OH/O<sup>-</sup>) in aqueous solution. *J. Phys. Chem.* 17, 513–886. <https://doi.org/10.1063/1.555805>.
- Chattaraj, P.K., Roy, D.R., 2007. Update 1 of: electrophilicity index. *Chem. Rev.* 107, PR46–PR74. <https://doi.org/10.1021/cr078014b>.
- Choi, D., Lee, O.-M., Yu, S., Jeong, S.-W., 2010. Gamma radiolysis of alachlor aqueous solutions in the presence of hydrogen peroxide. *J. Hazard Mater.* 184, 308–312. <https://doi.org/10.1016/j.jhazmat.2010.08.037>.
- Chu, L., Wang, J., Chen, C., He, S., Wojnárovits, L., Takács, E., 2021. Advanced treatment of antibiotic wastewater by ionizing radiation combined with peroxymonosulfate/H<sub>2</sub>O<sub>2</sub> oxidation. *J. Clean. Prod.* 321, 128921. <https://doi.org/10.1016/j.jclepro.2021.128921>.
- Dwinandha, D., Zhang, B., Fujii, M., 2022. Prediction of reaction mechanism for OH radical-mediated phenol oxidation using quantum chemical calculation. *Chemosphere* 291, 132763. <https://doi.org/10.1016/j.chemosphere.2021.132763>.
- Egerić, M., Matović, L., Savić, M., Stanković, S., Wu, Y., Li, F., Vujasin, R., 2024. Gamma irradiation induced degradation of organic pollutants: recent advances and future perspective. *Chemosphere* 352, 141437. <https://doi.org/10.1016/j.chemosphere.2024.141437>.
- Feng, L., Oturan, N., van Hullebusch, E.D., Esposito, G., Oturan, M.A., 2014. Degradation of anti-inflammatory drug ketoprofen by electro-oxidation: comparison of electro-Fenton and anodic oxidation processes. *Environ. Sci. Pollut. Res.* 21, 8406–8416. <https://doi.org/10.1007/s11356-014-2774-2>.
- Fitoz, A., Yılmaz, H., Hayvalı, M., Emregül, K.C., 2023. Evaluation of an aza dipyrromethene derivative as a green corrosion inhibitor via experimental and theoretical methods. *J. Mol. Liq.* 391, 123407. <https://doi.org/10.1016/j.molliq.2023.123407>.
- Frisch, M.J., Trucks, G.W., Schlegel, H.B., Scuseria, G.E., Robb, M.A., Cheeseman, J.R., Scalmani, G., Barone, V., Mennucci, B., Petersson, G.A., Nakatsuji, H., Caricato, M., Li, X., Hratchian, H.P., Izmaylov, A.F., Bloino, J., Zheng, G., Sonnenberg, J.L., Hada, M., Ehara, M., Toyota, K., Fukuda, R., Hasegawa, J., Ishida, M., Nakajima, T., Honda, Y., Kitao, O., Nakai, H., Vreven, T., Montgomery Jr., J.A., Peralta, J.E., Ogliaro, F., Bearpark, M., Heyd, J.J., Brothers, E., Kudin, K.N., Staroverov, V.N., Kobayashi, R., Normand, J., Raghavachari, K., Rendell, A., Burant, J.C., Iyengar, S.S., Tomasi, J., Cossi, M., Rega, N., Millam, J.M., Klene, M., Knox, J.E., Cross, J.B., Bakken, V., Adamo, C., Jaramillo, J., Gomperts, R., Stratmann, R.E., Yazyev, O., Austin, A.J., Cammi, R., Pomelli, C., Ochterski, J.W., Martin, R.L., Morokuma, K., Zakrzewski, V.G., Voth, G.A., Salvador, P., Dannenberg, J.J., Dapprich, S., Daniels, A.D., Farkas, O., Foresman, J.B., Ortiz, J.V., Cioslowski, J., Fox, D.J., 2009. Gaussian 09, Revision A.02. Gaussian, Inc., Wallingford, CT.
- Gao, H.P., Chen, J.B., Zhang, Y.L., Zhou, X.F., 2016. Sulfate radicals induced degradation of Triclosan in thermally activated persulfate system. *Chem. Eng. J.* 306, 522–530. <https://doi.org/10.1016/j.cej.2016.07.080>.
- Gao, Y., Ji, Y., Li, G., An, T., 2014. Mechanism, kinetics and toxicity assessment of OH-initiated transformation of triclosan in aquatic environments. *Water Res.* 49, 360–370. <https://doi.org/10.1016/j.watres.2013.10.027>.
- Genç, A., Ergun, E., Kantöglü, Ö., Ince, M., Acar, O., 2024. A realistic approach to radiation-induced treatment of micropollutants in wastewater. *Chem. Pap.* 78, 1415–1434. <https://doi.org/10.1007/s11696-023-03168-6>.
- He, J., Ye, Q., Zhu, Y., Yang, M., Zhao, L., 2023. Enhanced degradation performance and mineralization of ciprofloxacin by ionizing radiation combined with g-C<sub>3</sub>N<sub>4</sub>/CDs. *Radiat. Phys. Chem.* 208, 110958. <https://doi.org/10.1016/j.radphyschem.2023.110958>.
- Hina, H., Nafees, M., Ahmad, T., 2021. Treatment of industrial wastewater with gamma irradiation for removal of organic load in terms of biological and chemical oxygen demand. *Heliyon* 7 (2), e05972. <https://doi.org/10.1016/j.heliyon.2021.e05972>.
- Homlok, R., Takács, E., Wojnárovits, L., 2011. Elimination of diclofenac from water using irradiation technology. *Chemosphere* 85, 603–608. <https://doi.org/10.1016/j.chemosphere.2011.06.101>.
- Huang, D., Wang, Z., Zhang, J., Feng, J., Zheng, Z., Zhang, J., 2016. Gamma radiolytic degradation of 3,4-dichloroaniline in aqueous solution. *Sep. Purif. Technol.* 170, 264–271. <https://doi.org/10.1016/j.seppur.2016.06.052>.
- Huo, Z., Wang, S., Zou, Q., Shao, H., Xu, G., 2021. Radiolysis of cardiovascular drug atenolol in aqueous solution by electron beam: effect of water components and persulfate addition. *Radiat. Phys. Chem.* 184, 109458. <https://doi.org/10.1016/j.radphyschem.2021.109458>.
- Ibrahim, K.E.A., Elbashir, A.A., Ahmed, M.M.O., Şolpan, D., 2018. Radiolytic degradation of carbofuran by using gamma and gamma/hydrogen peroxide processes. *Radiat. Phys. Chem.* 153, 251–257. <https://doi.org/10.1016/j.radphyschem.2018.10.014>.
- Illés, E., Szabó, E., Takács, E., Wojnárovits, L., Dombi, A., Gajda-Schrantz, K., 2014. Ketoprofen removal by O<sub>3</sub> and O<sub>3</sub>/UV processes: kinetics, transformation products and ecotoxicity. *Sci. Total Environ.* 472, 178184. <https://doi.org/10.1016/j.scitotenv.2013.10.119>.
- Illés, E., Takács, E., Dombi, A., Gajda-Schrantz, K., Gonter, K., Wojnárovits, L., 2012. Radiation induced degradation of ketoprofen in dilute aqueous solution. *Radiat. Phys. Chem.* 81, 1479–1483. <https://doi.org/10.1016/j.radphyschem.2011.11.038>.
- Illés, E., Takács, E., Dombi, A., Gajda-Schrantz, K., Rácz, G., Gonter, K., Wojnárovits, L., 2013. Hydroxyl radical induced degradation of ibuprofen. *Sci. Total Environ.* 447, 286–292. <https://doi.org/10.1016/j.scitotenv.2013.01.007>.
- Iqbal, M., Bhatti, I.A., 2015. Gamma radiation/H<sub>2</sub>O<sub>2</sub> treatment of a nonylphenol ethoxylates: degradation, cytotoxicity, and mutagenicity evaluation. *J. Hazard Mater.* 299, 351–360. <https://doi.org/10.1016/j.jhazmat.2015.06.045>.
- Jia, L., Shen, Z., Su, P., 2016. Relationship between reaction rate constants of organic pollutants and their molecular descriptors during Fenton oxidation and in situ formed ferric-oxyhydroxides. *J. Environ. Sci.* 43, 257–264. <https://doi.org/10.1016/j.jes.2015.10.019>.
- Jia-Tong, L., Yong-Sheng, L., Qing, S., Da-Qian, H., Dan, Z., Wen-Bao, J., 2017. The treatment of aniline in aqueous solutions by gamma irradiation. *J. Adv. Oxid. Technol.* 20, 20160173. <https://doi.org/10.1515/jaots-2016-0173>.
- Kantöglü, Ö., Ergun, E., 2015. Degradation of morphine and codeine by gamma radiation in methanol solution. *Radiochim. Acta* 103, 137–147. <https://doi.org/10.1515/ract-2014-2284>.
- Kantöglü, Ö., Ergun, E., 2016. Radiation induced destruction of thebaine, papaverine and noscapine in methanol. *Radiat. Phys. Chem.* 124, 184–190. <https://doi.org/10.1016/j.radphyschem.2015.10.013>.
- Keen, O.S., McKay, G., Mezyk, S.P., Linden, K.G., Rosario-Ortiz, F.L., 2014. Identifying the factors that influence the reactivity of effluent organic matter with hydroxyl radicals. *Water Res.* 50, 408–419. <https://doi.org/10.1016/j.watres.2013.10.049>.
- Liu, Q., Luo, X., Zheng, Z., Zheng, B., Zhang, J., Zhao, Y., Yang, X., Wang, J., Wang, L., 2011. Factors that have an effect on degradation of diclofenac in aqueous solution by gamma ray irradiation. *Environ. Sci. Pollut. Res.* 18, 1243–1252. <https://doi.org/10.1007/s11356-011-0457-9>.
- Liu, Y., Mekic, M., Carena, L., Vione, D., Gligorovski, S., Zhang, G., Jin, B., 2020. Tracking photodegradation products and bond-cleavage reaction pathways of triclosan using ultra-high resolution mass spectrometry and stable carbon isotope analysis. *Environ. Pollut.* 264, 114673. <https://doi.org/10.1016/j.envpol.2020.114673>.
- Martínez, C., Vilarino, S., Fernández, M.I., Faria, J., Canle, L.M., Santaballa, J.A., 2013. Mechanism of degradation of ketoprofen by heterogeneous photocatalysis in aqueous solution. *Appl. Catal., B* 142–143, 633–646. <https://doi.org/10.1016/j.apcatb.2013.05.018>.
- Martínez-Araya, J., Salgado-Morán, G., Glossman-Mitnik, D., 2013. Computational nanochemistry report on the oxoams conceptual DFT indices and chemical reactivity. *J. Phys. Chem. B* 117, 6339–6351. <https://doi.org/10.1021/jp400241q>.
- Martínez-Araya, J.I., 2015. Why is the dual descriptor a more accurate local reactivity descriptor than Fukui functions? *J. Math. Chem.* 53, 451–465. <https://doi.org/10.1007/s10910-014-0437-7>.
- Melin, J., Ayers, P., Ortiz, J., 2007. Removing electrons can increase the electron density: a computational study of negative Fukui functions. *J. Phys. Chem. A* 111, 10017–10019. <https://doi.org/10.1021/jp075573d>.
- Miranda, M.O., Cavalcanti, W.E.C., Barbosa, F.F., de Sousa, J.A., da Silva, F.I., Pergher, S. B.C., Braga, T.P., 2021. Photocatalytic degradation of ibuprofen using titanium oxide: insights into the mechanism and preferential attack of radicals. *RSC Adv.* 11, 27720–27733. <https://doi.org/10.1039/D1RA04340D>.

- Munoz, M., de Pedro, Z.M., Casas, J.A., Rodriguez, J.J., 2012. Triclosan breakdown by Fenton-like oxidation. *Chem. Eng. J.* 198–199, 275–281. <https://doi.org/10.1016/j.cej.2012.05.097>.
- Nisar, J., Sayed, M., Khan, F.U., Khan, H.M., Iqbal, M., Khan, R.A., Anas, M., 2016. Gamma – irradiation induced degradation of diclofenac in aqueous solution: kinetics, role of reactive species and influence of natural water parameters. *J. Environ. Chem. Eng.* 4, 2573–2584. <https://doi.org/10.1016/j.jece.2016.04.034>.
- Oturan, M.A., Pinson, J., Bizot, J., Deprez, D., Terlain, B., 1992. Reaction of inflammation inhibitors with chemically and electrochemically generated hydroxyl radicals. *J. Electroanal. Chem.* 334, 103–109. [https://doi.org/10.1016/0022-0728\(92\)80563-J](https://doi.org/10.1016/0022-0728(92)80563-J).
- Pal, R., Chattaraj, P.K., 2023. Electrophilicity index revisited. *J. Comput. Chem.* 44, 278–297. <https://doi.org/10.1002/jcc.26886>.
- Parr, R.G., Yang, W., 1984. Density functional approach to the frontier-electron theory of chemical reactivity. *J. Am. Chem. Soc.* 106, 4049–4050. <https://doi.org/10.1021/ja00326a036>.
- Pucci, R., Angilella, G.G.N., 2022. Density functional theory, chemical reactivity, and the Fukui functions. *Found. Chem.* 24, 59–71. <https://doi.org/10.1007/s10698-022-09416-z>.
- Rath, M.C., Keny, S.J., Upadhyaya, H.P., Adhikari, S., 2023. Free radical induced degradation and computational studies of hydroxychloroquine in aqueous solution. *Radiat. Phys. Chem.* 206, 110785. <https://doi.org/10.1016/j.radphyschem.2023.110785>.
- Sakr, M.A.S., Sherbiny, F.F., El-Etrawy, A.A.S., 2022. Hydrazone-based materials; DFT, TD-DFT, NBO analysis, fukui function, MESP analysis, and solar cell applications. *J. Fluoresc.* 32, 1857–1871. <https://doi.org/10.1007/s10895-022-03000-6>.
- Shah, N.S., Khan, J.A., Sayed, M., Khan, Z.U.H., Iqbal, J., Arshad, S., Junaid, M., Khan, H. M., 2020. Synergistic effects of H<sub>2</sub>O<sub>2</sub> and S<sub>2</sub>O<sub>8</sub><sup>2-</sup> in the gamma radiation induced degradation of Congo-red dye: kinetics and toxicities evaluation. *Sep. Purif. Technol.* 233, 115966. <https://doi.org/10.1016/j.seppur.2019.115966>.
- Song, Z., Wang, N., Zhu, L., Huang, A., Zhao, X., Tang, H., 2012. Efficient oxidative degradation of triclosan by using an enhanced Fenton-like process. *Chem. Eng. J.* 198–199, 379–387. <https://doi.org/10.1016/j.cej.2012.05.067>.
- Szabó, R.K., Megyeri, Cs, Illés, E., Gajda-Schrantz, K., Mazellier, P., Dombi, A., 2011. Phototransformation of ibuprofen and ketoprofen in aqueous solutions. *Chemosphere* 84, 1658–1663. <https://doi.org/10.1016/j.chemosphere.2011.05.012>.
- Wang, J., Chu, L., 2016. Irradiation treatment of pharmaceutical and personal care products (PPCPs) in water and wastewater: an overview. *Radiat. Phys. Chem.* 125, 56–64. <https://doi.org/10.1016/j.radphyschem.2016.03.012>.
- Wang, J., Zhuan, R., Chu, L., 2019. The occurrence, distribution and degradation of antibiotics by ionizing radiation: an overview. *Sci. Total Environ.* 646, 1385–1397. <https://doi.org/10.1016/j.scitotenv.2018.07.415>.
- Wang, S.Z., Yin, Y.N., Wang, J.L., 2017. Enhanced biodegradation of triclosan by means of gamma irradiation. *Chemosphere* 167, 406–414. <https://doi.org/10.1016/j.chemosphere.2016.10.028>.
- Wojnárovits, L., Takács, E., 2016. Radiation induced degradation of organic pollutants in waters and wastewaters. *Top. Curr. Chem.* 374, 50. <https://doi.org/10.1007/s41061-016-0050-2>.
- Woods, R.J., Pikaev, A.K., 1994. *Applied Radiation Chemistry: Radiation Processing*, first ed. Wiley, New York.
- Yang, W., Mortier, W.J.J., 1986. The use of global and local molecular parameters for the analysis of the gas-phase basicity of amines. *Am. Chem. Soc.* 108, 5708–5711. <https://doi.org/10.1021/ja00279a008>.
- Yu, H., Nie, E., Xu, J., Yan, S., Cooper, W.J., Song, W., 2013. Degradation of diclofenac by advanced oxidation and reduction processes: kinetic studies, degradation pathways and toxicity assessments. *Water Res.* 47, 1909–1918. <https://doi.org/10.1016/j.watres.2013.01.016>.
- Yu, S., Hu, J., Wang, J., 2010. Gamma radiation-induced degradation of p-nitrophenol (PNP) in the presence of hydrogen peroxide (H<sub>2</sub>O<sub>2</sub>) in aqueous solution. *J. Hazard Mater.* 177, 1061–1067. <https://doi.org/10.1016/j.jhazmat.2010.01.028>.
- Zamora, P.P., Bieger, K., Cuchillo, A., Tello, A., Mueña, J.P., 2021. Theoretical determination of a reaction intermediate: fukui function analysis, dual reactivity descriptor and activation energy. *J. Mol. Struct.* 1227, 129369. <https://doi.org/10.1016/j.molstruc.2020.129369>.
- Zhang, Z., Hu, D., Chen, H., Chen, C., Zhang, Y., He, S., Wang, J., 2021. Enhanced degradation of triclosan by gamma radiation with addition of persulfate. *Radiat. Phys. Chem.* 180, 109273. <https://doi.org/10.1016/j.radphyschem.2020.109273>.
- Zheng, B.G., Zheng, Z., Zhang, J.B., Luo, X.Z., Wang, J.Q., Liu, Q., Wang, L.H., 2011. Degradation of the emerging contaminant ibuprofen in aqueous solution by gamma irradiation. *Desalination* 276, 379–385. <https://doi.org/10.1016/j.desal.2011.03.078>.
- Zhuan, R., Wang, J., 2020. Degradation of diclofenac in aqueous solution by ionizing radiation in the presence of humic acid. *Sep. Purif. Technol.* 234, 116079. <https://doi.org/10.1016/j.seppur.2019.116079>.